

DESIGN OF A FULL C-BAND INJECTOR FOR ULTRA-HIGH BRIGHTNESS ELECTRON BEAM

D. Alesini, G. Castorina, M. Croia, M. Ferrario, A. Gallo, B. Spataro, C. Vaccarezza, A. Vannozzi,
 INFN-LNF, Frascati, Italy

M. Diomede, INFN-LNF, Frascati, Italy and University of Rome “La Sapienza”, Rome, Italy

A. Giribono, F. Cardelli, ENEA, Frascati, Italy

Abstract

High gradient rf photo-injectors have been a key development to enable several applications of high quality electron beams. They allow the generation of beams with very high peak current and low transverse emittance, satisfying the tight demands for free-electron lasers, energy recovery linacs, Compton/Thomson sources and high-energy linear colliders. In the paper we present the design of a new full C-band RF photo-injector recently developed in the framework of the XLS-Compact Light design study and of the EuPRAXIA@SPARC_LAB proposal. It allows to reach extremely good beam performances in terms of beam emittance (at the level of few hundreds nm), energy spread and peak current. The photo-injector is based on a very high gradient (>200 MV/m) ultra-fast (RF pulses <200 ns) C-band RF gun, followed by two C band TW structures. Different types of couplers for the 1.6 cell RF gun have been considered and also a new compact low pulsed heating coupler working on the TM_{020} mode on the full cell has been proposed. In the paper we report the design criteria of the gun, the powering system, and the results of the beam dynamics simulations. We also discuss the case of 1 kHz repetition rate.

INTRODUCTION

RF photo-guns [1] find applications as injectors for FELs, THz and Compton sources and electron diffraction [2-15] allowing reaching very high beam brightness. Since the peak field at the cathode (E_{cath}) is proportional to the achievable beam brightness [16], in the last generation of RF guns a great effort has been put to increase the field amplitude, and, at the same time, to reduce breakdown rate probability (BDR) [17]. On the other hand, the possibility to operate such a gun in the kHz regime is very attractive for all mentioned applications. Moreover, in the context of the X-band linacs of the EuPRAXIA@SPARC_LAB proposal [18] and XLS design study [19] the possibility to implement a full C-band injector is attractive for both reachable beam parameters and compactness.

The schematic layout of the full C-band injector we are proposing is given in Fig. 1. The C-band gun is followed by two C-band TW structures that we have scaled, to the first order, by those developed for the SwissFeL [20] and that can operate with a single klystron and a pulse compressor at the level of 40 MV/m. The solenoids after the gun and around the TW structures allow to keep under control the beam emittance increase also in case of longitudinal compression by velocity bunching [21]. The correct scaling laws for the cathode field [16], indicate that, in order to gain in term of emittance and brightness

one has to scale $E_{cath} \propto \lambda_{RF}^{-1}$. This drives to the conclusion that, in C-band, if we want to scale the working points of the S band guns we have to reach a cathode peak field of 240 MV/m. The design of the gun is focused to achieve such a high gradient keeping under control all known quantities that drive the breakdown phenomena.

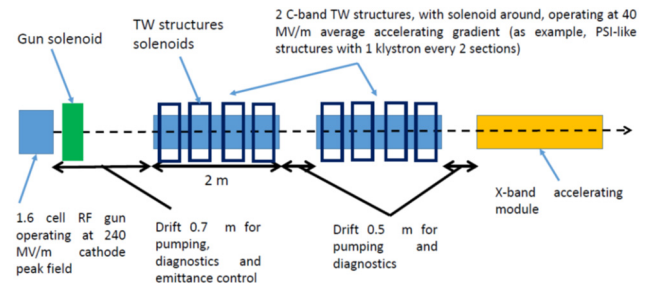


Figure 1: Schematic layout of the C-band injector.

Table 1: Main Parameters of the C-band Gun (the values in parenthesis are referred to the TM_{020} -type coupler)

Parameter	value
Resonant frequency	5.712
$E_{cath}/\sqrt{P_{diss}}$ [MV/(m·MW ^{0.5})]	65 (55)
RF input power [MW]	40 (70)
Cathode peak field [MV/m]	200-240
Rep. rate [Hz]	100-1000
Quality factor	11000 (14000)
Filling time [ns]	150
Coupling coefficient	3
RF pulse length [ns]	180
Mode separation $0-\pi$ [MHz]	~ 90
E_{surf}/E_{cath}	0.9
Pulsed heating [°C]	<40
Average diss. Power [W]	200-2000

DESIGN CRITERIA OF THE GUN

In the design of the gun we have considered that, according to the high gradient test performed on X-band structures, there are three main quantities that allow to control and predict, in principle, the final BDR in a radiofrequency (RF) structure. Such a quantities are: the peak E field (E_{cath}), the modified Poynting vector (S_c) [22], the RF pulse length (t_p) and Pulsed Heating (ΔT) [23]. In particular, if $E_{cath} \leq 240$ MV/m, $t_p \leq 180$ ns, $S_c \leq 6$ W/ μm^2 and $\Delta T \leq 40^\circ C$, the expected BDR is less than 2×10^{-6} bpp [24]. The two quantities S_c and ΔT can be kept below these values with a proper design of the cells and couplers, while short RF pulses can be used if we increase the input peak

Content from this work may be used under the terms of the CC BY 3.0 licence (© 2019). Any distribution of this work must maintain attribution to the author(s), title of the work, publisher, and DOI

power and if we properly choose of the coupling coefficient (β). The optimized 2D profile of the gun with main dimensions are given in Fig. 2 while its main parameters are reported in Table 1.

The required input and reflected powers as a function of β and for different pulse lengths are given in Fig. 3. We have finally fixed $\beta=3$, an input power of 40 MW and a pulse length of 180 ns.

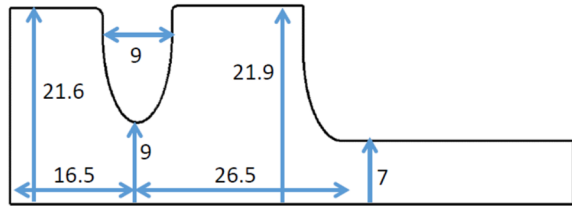


Figure 2: 2D gun profile with main dimensions (in mm).

Standard couplers on the full cell, even if strongly rounded [25,26] cannot be used because of the high magnetic field and, as a consequence, high pulsed heating on the coupling holes. For this reason, two different solutions have been explored and are schematically represented in Fig. 4. The first type of coupler is a mode launcher-type coupler [27] while the second one is a new coupler we have proposed that operate on the TM_{020} mode on the full cell. This allow to couple the field in the waveguide, electrically, strongly reducing the pulsed heating. There are advantages and disadvantages in the two solutions. In particular, the second type of coupler allows to use a solenoid immediately after the gun simply scaled from S-band guns. On the contrary the mode launcher one needs the development of a new solenoid with large bore and bucking coils to cancel the magnetic field on the cathode. The first type of coupler shows also a larger ratio $E_{cath}/\sqrt{P_{diss}}$ and is mechanically more simple, it also allows a better and uniform cooling of the accelerating cells.

Concerning the feeding system, two possible solutions are schematically represented in Fig. 5. Commercial circulators, able to handle 50 MW input/reflected power, already exist in C-band [28] and also pulse compressors that can manage up to 300 MW output power have been developed in C-band [29]. The second proposed scheme is more flexible and allows, in principle, to explore even shorter pulses.

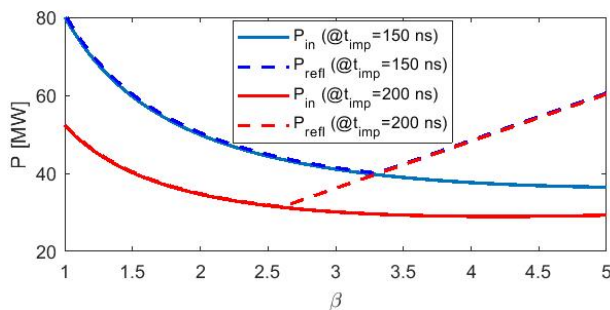


Figure 3: Required input and reflected powers as a function of β and for different pulse lengths.

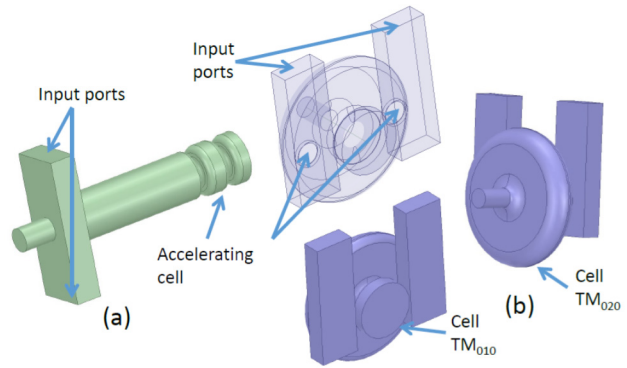


Figure 4: Proposed input couplers: (a) mode launcher type; (b) new coupler with TM_{020} cell.

OPERATION AT REP. RATE OF 1 kHz

A strong interest in the last photo-injector generation is the possibility to operate at the kHz regime and also in the context of the XLS design study this possibility is under consideration for the soft X-ray case. The high repetition rate operation is limited by two effects: the average dissipated power in the structure and the klystron available power. It is relatively easy to demonstrate that, because of the short RF pulses, the average dissipated power in the gun, even at the maximum gradient, is below 2 kW and can be managed. Of more concern is the second limitation given by the maximum power can be released on the klystron collector. Considering typical klystron parameters in C-band [30] it is possible to estimate the maximum available power at different repetition rates and pulse lengths keeping constant the average dissipated power on the collector. The results in terms of reachable cathode field are reported in Fig. 6 where we also reported the average dissipated power in the gun. These first results clearly shown that the kHz operation is, at least, feasible even with commercial and not optimized klystrons.

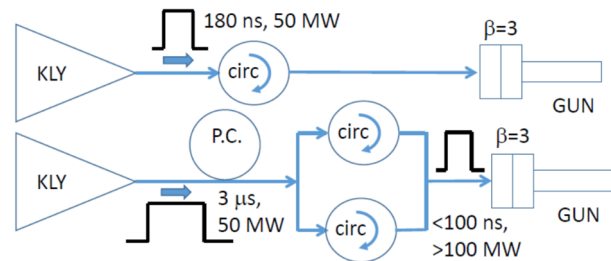


Figure 5: possible feeding systems.

BEAM DYNAMICS SIMULATIONS

The working point of the injector has been scaled from the well-known S-band injectors. To this purpose the longitudinal lengths of the devices (cavities and magnets) have been scaled by a factor two and the fields (electric and magnetic) have been doubled with respect to the S-band case. We used the simulation code GPT [31] with 20k particles for fast parameters scans while the final simulations have been done using 250k particles.

The laser parameters have been scaled using the formula reported in [16] to have the same bunch charge density of

the LCLS and SPARC_LAB cases [32-35] adopting the same emittance compensation technique. The intrinsic emittance [36,37] has been calculated, for the copper cathode, considering the ideal case of a flat cathode (i.e. field enhancement factor $\beta_{rf} \approx 1$) giving $\epsilon_{int} \approx 0.8 \mu\text{m}/\text{mm}$.

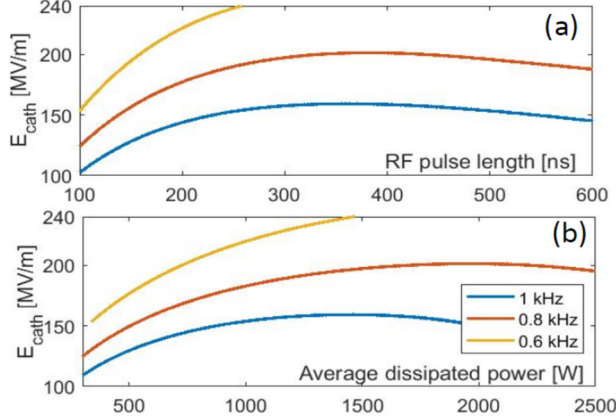


Figure 6: (a) cathode E-field at different rep. rate and pulse lengths; (b) corresponding average dissipated power.

We have analysed the two cases of on crest acceleration and longitudinal compression using the velocity bunching technique [38], to match the XLS requirements. In this second case the solenoids around the two C-band structures have been tuned to keep under control the spot size and the emittance. The final normalized emittance on crest and in the compression case are the same and equal to $\epsilon_{n,rms} \approx 0.15 \mu\text{m}$.

Figs. 7 and 8 show the evolution of the main beam parameters along the injector itself while Table 2 summarize the beam parameters at the end of injector in the two cases. One of the main advantages of this high gradient gun is to quickly freeze the emittance after the cathode, dumping in a shorter distance, the space charge forces. This is important to reduce the non-linear space charge contribution to the emittance that cannot be reduced using the emittance compensation scheme. Moreover, the beam at the exit of the injector can be directly injected into X-band modules.

Table 2: Main Beam and Laser Parameters at the End of Injector in Two Cases: with and w/o Bunch Compression

Parameter	w/o BC	with BC
Laser spot size [μm]	294 (uniform)	
Laser rms length [ps]	3.4	
Rise time laser pulse [fs]	600	
Bunch charge [pC]	75	
Beam emittance [mm-mrad]	0.15	
Bunch length [μm]	295	105
Beam Energy [MeV]	170	107
Peak current [A]	22	60
Beam energy spread [%]	0.6	1.4

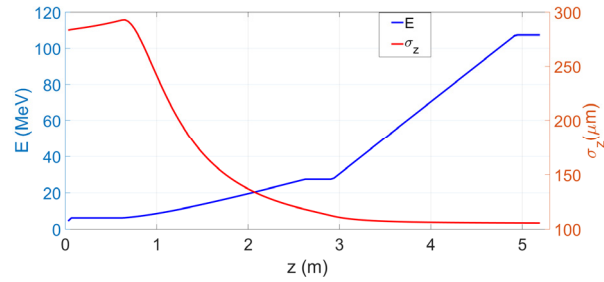


Figure 7: Evolution of the beam energy and bunch length along the C-band injector.

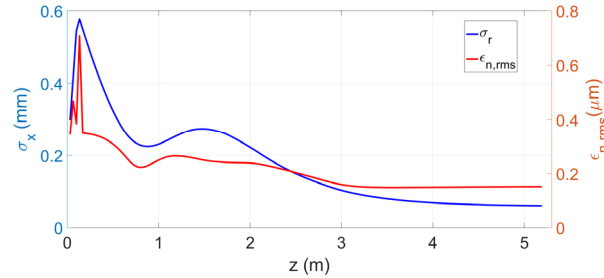


Figure 8: Evolution of the beam envelope and emittance along the C-band injector.

CONCLUSIONS

The design of a full C-band injector has been illustrated. The injector is based on a 1.6 cell high gradient RF gun operating at 240 MV/m cathode peak field fed by extremely short pulses and followed by two TW C-band structures. The design criteria of the gun have been discussed and two options for the coupling system have been shown. The first is based on a mode launcher coupler while the second on a new design in which the full cell operate on the TM_{020} mode and the rectangular waveguide is electrically coupled to the cell. Preliminary considerations on the 1 kHz rep. rate regime have been done showing the feasibility of this type of operation. Beam dynamics simulations have been also performed and clearly indicate that the performances of this type of injector are challenging and perfectly match the requirements of the XLS and EuPRAXIA@SPARC_LAB projects.

ACKNOWLEDGEMENTS

The work has been partially supported by the European Union's Horizon 2020 research and innovation programme under grant agreement No 777431. We would like also to thank Dr. Toshiro Anno for the helpful discussion, technical suggestions and information on high rep. rate klystron operation.

REFERENCES

- [1] D. Palmer, “The next Generation Photoinjector”, Ph.D. thesis, June 1998.
- [2] P.G. O’Shea *et al.*, in *Proc. 1991 IEEE Particle Accelerator Conference*, 1991, p. 2754.
- [3] D.H. Dowell *et al.*, *Appl. Phys. Lett.* 63 (1993) 2035.
- [4] R. Dei-Cas *et al.*, *Nucl. Instr. and Meth. A* 296 (1990) 209.
- [5] S. Schreiber, in *Proc. the European Particle Accelerator Conference*, 2000, p. 309.
- [6] R. Akre *et al.*, *Phys. Rev. ST Accel. Beams* 11 (2008) 030703.
- [7] H.S. Kang, S.H. Nam, in *Proc. FEL’10*, 2010, p. 155.
- [8] R. Kuroda, *Nucl. Instr. and Meth. A* 593 (2008) 91.
- [9] C. Yim *et al.*, in *Proc. IPPAC’10*, 2010, p. 1059.
- [10] J.B. Hasting *et al.*, *Appl. Phys. Lett.* 89 (2006) 184109.
- [11] R. Li *et al.*, *Rev. Sci. Instrum.* 80 (2009) 083303.
- [12] J. Yang *et al.*, *Rad. Phys. Chem.* 78 (2009) 1106.
- [13] P. Musumeci *et al.*, *Rev. Sci. Instrum.* 82 (2010) 013306.
- [14] J.-H. Han, *Phys. Rev. ST Accel. Beams* 14 (2011) 050101.
- [15] R. Kuroda *et al.*, *Nucl. Instr. and Meth. A* 637 (2011) S183.
- [16] J.B. Rosenzweig, E. Colby, TESLA-95-04.
- [17] V.A. Dolgashev *et al.*, “RF breakdown in normal conducting single-cell structures”, in *Proc. PAC’05*, May 16–20, Knoxville, Tennessee, U.S.A. (2005).
- [18] M. Ferrario *et al.*, “Design study towards a compact FEL facility at LNF”, EuPRAXIA@SPARC_LAB, arXiv:1801.08717.
- [19] <http://www.compactlight.eu/Main/HomePage>
- [20] R. Zennaro *et al.*, *Proc. LINAC’14*, p. 333, 2014.
- [21] M. Ferrario *et al.*, “Experimental demonstration of emittance compensation with velocity bunching”, *Physical review letters*, 104(5):054801, 2010.
- [22] A. Grudiev *et al.*, *PRST-AB* 12, 102001 (2009)
- [23] V. A. Dolgashev, *PAC 2003*, p. 1267.
- [24] W. Wuensch, in *Proc. IPAC’17*, 2017.
- [25] C. Limborg *et al.*, Report No. LCLS-TN-05-3.
- [26] D. Alesini *et al.*, *gun eli PRAB* 21, 112001 (2018).
- [27] C. Nantista *et al.*, “Low-field accelerator structure couplers and design techniques”, *Phys. Rev. ST Accel. Beams* 7 (2004) 072001.
- [28] <https://www.cmlengineering.com/>
- [29] R. Zennaro *et al.*, in *Proc. IPAC2013*, p. 2827.
- [30] Toshiro Anno (Canon) private communications.
- [31] General Particle Tracer, <http://www.pulsar.nl/gpt/>
- [32] Arthur, J. *et al.*, “Linac coherent light source (LCLS) conceptual design report”, No. SLAC-0593. 2002.
- [33] B.E. Carlsten, “New photoelectric injector design for the Los Alamos National Laboratory XUV FEL accelerator”, *Nucl. Instr. and Meth. in Physics Research A: Accelerators, Spectrometers, Detectors and Associated Equipment* 285.1-2 (1989): 313-319.
- [34] M. Ferrario *et al.*, “HOMDYN study for the LCLS RF photo-injector”, *The Physics of High Brightness Beams* 2000 534-563.
- [35] M. Ferrario *et al.*, “Direct measurement of the double emittance minimum in the beam dynamics of the sparse high-brightness photoinjector”, *Physical review letters*, 99 (23) 234801, 2007.
- [36] D. H. Dowell and J. F. Schmerge, “Quantum efficiency and thermal emittance of metal photocathodes”, *Physical Review Special Topics-Accelerators and Beams*, 12 (7) 074201, 2009.
- [37] Graves, W. S. *et al.* “Measurement of thermal emittance for a copper photocathode”, in *Proc. PAC2001*, (Cat. No. 01CH37268). Vol. 3. IEEE, 2001.
- [38] M. Ferrario *et al.*, “Experimental demonstration of emittance compensation with velocity bunching”, *Physical review letters*, 104 (5) 054801, 2010.